Chemical Science

Accepted Manuscript

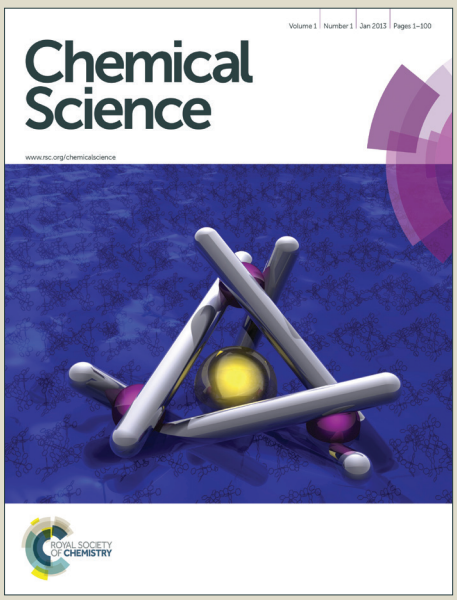

ROYAL SOCIETY OF CHEMISTRY

www.rsc.org/chemicalscience

Chemical Science

RSCPublishing

EDGE ARTICLE

Edge Overgrowth of Spiral Bimetallic Hydroxides Ultrathin-Nanosheets for Water Oxidation

Cite this: DOI: 10.1039/x0xx00000x

Bing Ni and Xun Wang*

Received,
Accepted

DOI: 10.1039/x0xx00000x

www.rsc.org/

Structures of edges may dramatically influence the properties of nanomaterials, so the rational design or control over the structures of edge is required. Here we synthesized spiral ultrathin-nanosheets with overgrown edges (SUNOE) of NiFe, CoNi and CoFe bimetallic hydroxides by governing the rates of different directions in screw dislocation driven growth (SDDG) in nonaqueous solvent. The driving force for SDDG is supersaturation, which could be controlled by the concentration of different precursors, thus achieving non-uniform structures of edges and inner sheets. NiFe, CoNi and CoFe bimetallic hydroxides possess layered structures, in which overgrown edges may prevent them from re-stacking. The as prepared SUNOE all show good performance for oxygen evolution reaction (OER) in electrolysis of water, and the lowest onset potential is 1.45V (vs RHE) (the lowest potential when current density reach 10 mA/cm^2 is 1.51 V (vs RHE)).

Introduction

Usually edges show unique properties other than faces in nanomaterials. For example, one of the central problems in field of graphene-related research is how it behaves with different edge structures[1-3]. Edges of transition-metal dichalcogenides (TMDs) possess different properties with inner sheets[4-7]. And increasing the content of atoms at the edges in noble metal nanoparticles would greatly enhance the catalytic properties[8]. To some extent, well-designed edges would give a promising future for nanomaterials' application. Spiral TMDs has been achieved in recent studies[9, 10], however, the edge structures of them are less studied. Spiral structure are usually achieved via screw dislocation driven growth (SDDG). The driving force for SDDG is supersaturation, which could be controlled by the concentration of different precursors, thus achieving non-uniform structures of edges and inner sheets.

In most cases, the edges of nanostructures are just the natural ends of faces of particles. Etching is a probable method to tune the environment around edges[11-13], this could be seen as a "top-down" method. It is always important to figure out diverse solutions for certain goals and bring much more possibilities. Herein we present a "bottom-up" solution to design the edges of nanosheets, by SDDG of crystals. SDDG is a classic graph to illustrate the crystal growth in low supersaturation[14, 15]. The crystal grows from a screw dislocation and enlarges with two competitive rates, one is in-plane rate, r_i, and the other is vertical rate, r_v[16-19]. We controlled these two rates by the concentrations of precursors in nonaqueous solvent, thus achieved the overgrowth of edges in ultralthin-nanosheets. The final morphologies are spiral ultrathin nanosheets with overgrown edges (SUNOE) (Figure 1, 2). The discernible spokewise edges indicate a SDDG mechanism. Edge overgrowth has shown power in the synthesis of nanoparticles enclosed by high index facets[20, 21], such strategy requires judicious control over precursors and surface chemistry. Herein the edge overgrowth driven by concentrations change during SDDG provides another easy accessible and highly controllable method to fabricate novel structures. As a proof of concept, the report here illustrates feasibility to prepare edge overgrowth in two dimensional materials.

Alpha phase of metal hydroxide species could possess layered structures similar with layered double hydroxides.[22, 23] We choose them as the research objects, not only because the rules studied here may extend to other cutting-edge research in layered structures, such as graphene, TMDs, but also because of the inherent differences in a-b direction with c direction, which we could utilize the different growth rates in a-b plane and vertical to a-b plane. Meanwhile, earth abundant hydroxides like NiFe layered double hydroxides are effective catalysts for OER[24, 25]. Water splitting is a hot topic for energy conversion and conservation[26]. For electrolysis of water, anodic overpotential is the main obstacle[27]. So exploring catalyst with low overpotential for OER is meaningful and valuable.

Results and discussion

In a typical synthesis, two metal salts were required, one was sulfate and the other was chloride, the ratio was optimized for different products. For all the salts containing water in their lattice, we could avoid adding extra water into the system. After salts were weighed and transferred into an autoclave, ethanol and oleylamine or octaylamine were injected. After sonicate

and adding hexane, the autoclave was sealed and put into an oven which was set at specific temperature and time (details in supporting information). X-ray diffraction (XRD) data, X-ray photoelectron spectroscopy (XPS) and Fourier Transform Infrared Spectrometer (FT-IR Spectrometer) data suggest alpha phase structures of of NiFe, CoNi and CoFe hydroxides with SO_4^{2-} intercalation (Figure S1, S2, S3).

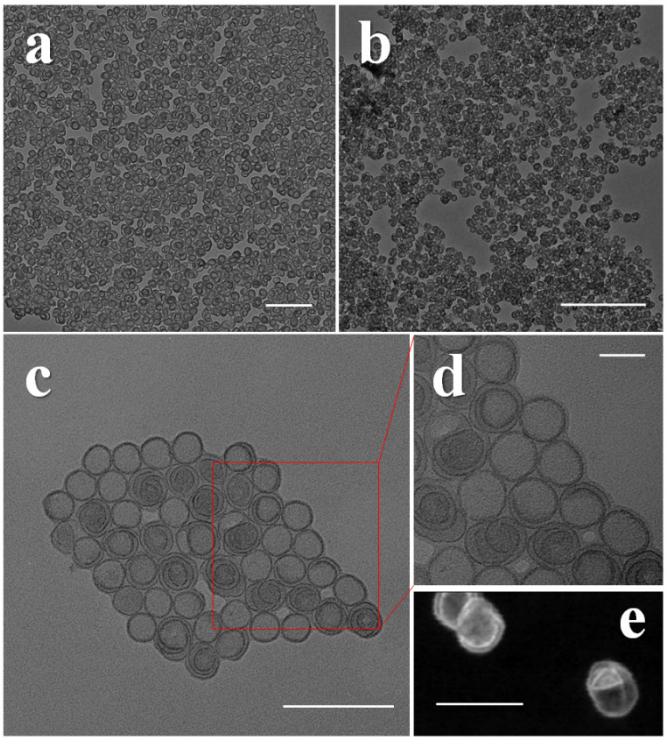

Figure 1 TEM images of CoNi (a), CoFe (b) and NiFe (c,d) SUNOE, the color of edges is darker than that of inner sheets; (e), STEM image of NiFe showing ultrathin spiral sheets structures, the ultrathin sheets could be folded. Scale bar: a, 200 nm; b, 500 nm; c, 100

As we can see in transmission electron microscopy (TEM) images, the final products are pure SUNOE (Figure 1, S4). The details of various SUNOE are studied in a higher magnification (Figure 1d, 2a, b, c) and high angle annular dark field scanning transmission electron microscopy (HAADF-STEM) (Figure 1e, 2d, f, g). The sheet diameters for all these three kinds SUNOE are about 30-50 nm, and the dark edges in the TEM image are about 1 nm. For NiFe SUNOE, there are two kinds of sheets with overgrown edges, one is single layer sheet and the other is spiral sheet. The single layer sheets may be formed due to the lack of screw dislocation or re-link of the stagger edges of spiral sheets. The edges of CoFe SUNOE are more likely to be in concentric circles, like growth rings in a tree. From STEM image (Figure 2d, f, g) or high resolution scanning electron microscopy (HRSEM) (Figure 2e), we can clearly see a spiral structure, and some of the sheets are broken or folded because of the ultrathin inherence. By taking account of all the aforementioned data, we can assure the products are layered spiral nanosheets with overgrown edges, and the SUNOE are grew in a screw dislocation driven way.

From TEM and STEM images, we can easily see the contrasts of edges and inner sheets are different. Then could there be different in chemical component of them? By using the energy dispersive spectroscopy line scan, we further investigated the differences between edges and inner sheets. For each kind of products, more than 10 single SUNOE were tested to get solid results, and all of them were highly consistent (Figure 2g, S5). For all such SUNOE, the ratio of metal to S (SO_4^{2-} by FT-IR) varies from inner sheets to edges, shows much higher value in the edges. The counts of S decrease at edges, while the counts of metals show a sudden increase in the edges. The peaks are broadened due to the drift of samples during tests. The results are same in all these three products, suggesting the edges are sudden enriched of hydroxides while the inner sheets keep growing as SDDG, showing an inherent growth mechanism of such SUNOE. The driving force for this transition may be concentration of SO_4^{2-}. Figure S6 portrait the products under different amounts of SO_4^{2-}, SUNOE could be obtained only under optimized concentration.

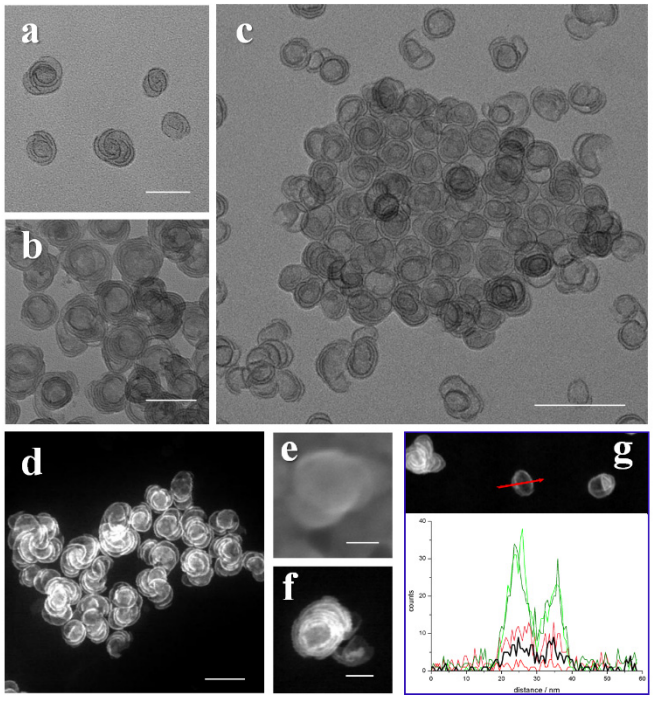

Figure 2 TEM images of SUNOE. The products of NiFe (a), CoFe (b) and CoNi (c) SUNOE with high purities; STEM image of NiFe (g), CoFe (f) and CoNi (d) SUNOE and HRSEM image of CoFe (e) SUNOE clearly showing spiral structure with overgrown edges; Energy dispersive spectroscopy line scan of NiFe SUNOE (g) suggesting composition difference in edges and inner sheets, in which the red arrow shows scan direction; Green line stands for Ni-K, olive line for Ni-L, red line for Fe-K, pink line for Fe-L and black line for S; The two peaks indicating higher metal contents in the edges. Scale bar: a, b, e, 50 nm; c, 200 nm; e, f, 20 nm.

The growth of SUNOE followed the mechanism as shown in Figure 3. The hydroxides are formed via dehydration of

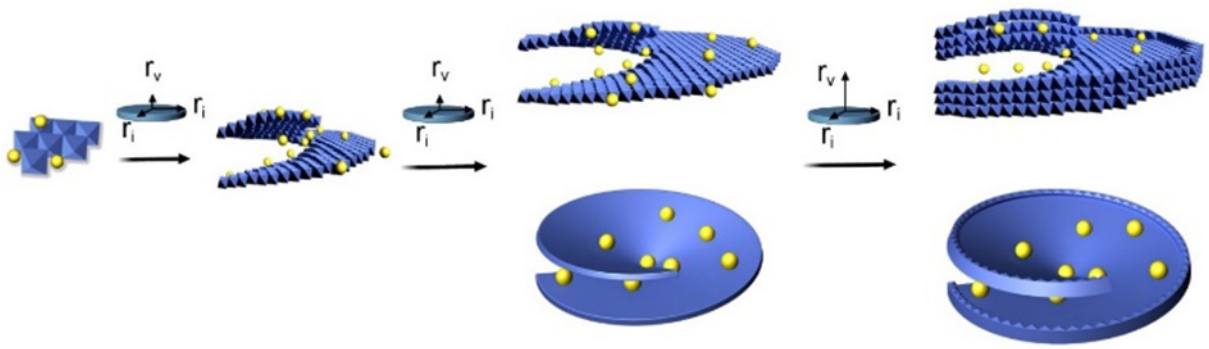

Figure 3 Proposed growth mechanism of SUNOE. At the beginning of the reaction, SO_4^{2-} and hetero-cation induce the formation of screw dislocation, SO_4^{2-} inhibit r_v dramatically, thus the sheets enlarge mainly in-plane, results in ultrathin sheets. When concentration stairs. In most cases of materials synthesis through SDDG, the concentration of precursors should be kept same to ensure that the growth simply follow SDDG during the whole reaction[16, 30], thus forming uniform and large enough particles. However, the edges would grow ordinarily in such method. The growth can be governed by competitive r_i and r_v, and these two rates determine the final morphology. Herein SO_4^{2-} inhibits both rates but stronger affect for r_v. A larger r_v would lead to more layers for the final products, lower ratio of r_v to r_i would lead to morphology of concentrate circles, like in CoFe SUNOE case. After the amount of SO_4^{2-} in reaction medium decrease to a critical level, r_v is released and cause overgrowth in growth sites, resulting in overgrowth in the edges. While at this time, the precursors have already consumed a lot, the sudden consumption here would lead to the fast run out of all precursors and terminate the enlargement. Role of other parameter was elaborated (Figure S8, S9, S10), solvent composition is as important as SO_4^{2-}, since solvent composition would influence supersaturation in the system, which is the driving force of SDDG. The requirements of such rule are simple and only need hetero ions to form screw dislocations and dissipative compounds to control the two growth rates, thus the rule could be further extended to other system with the consideration of practical parameters.

dissolved precursors. In this nonaqueous condition, the solvent molecule won't interfere the dehydration process of precursors, thus the reaction could happen in a relative mild condition comparing with that in aqueous solvent. Previous researches have shown that ultrathin hydroxides could be obtained by exfoliation of bulk hydroxides with the help of intercalations by various anions[28, 29]. In this "bottom-up" case, SO_4^{2-} could inhibit the stack of layers in a crystal way. In other words, the growth rate vertical to plane is dramatically hindered, thus the sheets are highly limited in vertical direction and form ultrathin structure. Meanwhile hetero-atoms would help to form screw dislocations[19]. Hetero metal ions are also important to form screw dislocations, altering the metal ratio would help to form uniform products (Figure S7).The screw dislocation would break flat structure, and make the sheets stagger like spiral

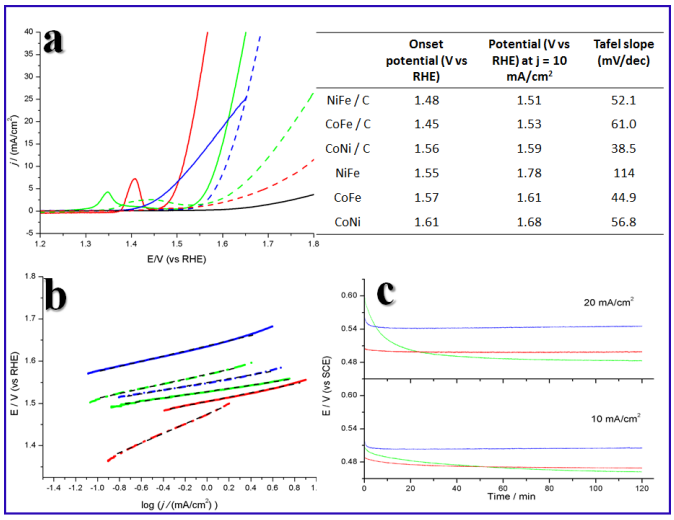

	Onset potential (V vs RHE)	Potential (V vs RHE) at j = 10 mA/cm²	Tafel slope (mV/dec)
NiFe / C	1.48	1.51	52.1
CoFe / C	1.45	1.53	61.0
CoNi / C	1.56	1.59	38.5
NiFe	1.55	1.78	114
CoFe	1.57	1.61	44.9
CoNi	1.61	1.68	56.8

Figure 4 OER properties of as prepared SUNOE. The red line stands for NiFe, blue line for CoFe and green line for CoNi, black for pure carbon (Vulcan XC72). Left in (a) is LSV graph for each sample, solid lines are products mixed with carbon, dash lines stand for sample without carbon. Tafel plots are draw in (b), solid line for products with carbon, dash and dot line for sample without carbon, black dash lines are fitting results. Chronopotential tests at 10 mA/cm^2 (c, below) and 20 mA/cm^2 (c, up) show a decrease of potential.

The as prepared SUNOE mixed with carbon (Vulcan XC72) all show good performances for OER. The linear sweep voltammetry (LSV) was applied to test the onset potential (Figure 4a, all data are without iR compensation). For pure SUNOE, the performances were ordinary in which the onset potentials range from 1.55 V to 1.61 V. However, when carbon was added to increase the conductivity of SUNOE, the onset potential showed a huge drop of 50 mV to 120 mV. The best material here is CoFe SUNOE with carbon which showed an onset potential at 1.45 V, better than the reported amorphous cobalt iron oxides[31]. Electrochemical surface area and conductivity are two main factors to increase the performances of catalyst[29]. The diameters of as prepared SUNOE are about 30-50 nm, it's reasonable to hold the point that electrons are difficult to conduct between different SUNOE, while introducing carbon would enhance the conductivity as well as

the activity of SUNOE (Figure S12). Meanwhile pure carbon didn't show activity for OER. The potential at j=10 mA/cm² is another important indicator for real use of solar energy and water splitting[32]. Here the SUNOE mixed with carbon showed potential down to 1.51 V, owed to NiFe SUNOE, comparable with the recent published efficient performance[33-35]. The smallest tafel slope here is 38.5 mV/dec, corresponding to CoNi SUNOE. Chronopotential test set current density at 10 and 20 mA/cm² were applied to evaluate the stabilities of as prepared materials (Figure 4c). The potential didn't increase, to the opposite, decreased, especially for CoNi SUNOE. The effect of anode treatment has been well studied by some groups[36, 37], and they suggested that after anode treatment, there would be more Co^{IV} species, while Co^{IV}-O is benifit for OER. We also examined the super capacitor performance of SUNOE (Figure S15), bubbles produced at the surface of electrode obviously while the potentials were still low. By calculating the charge stored before bubbling, we found that less than 25% of cations were oxidized. β-$Co(OH)_2$ ultrathin-nanosheets showed much higher specific capacitance than layered $Co(OH)_2$ for super capacitor application[38], surface segregation could stable Ru-Ir oxides with high OER activity[39], these enlightened us that the overgrown edges may increase and stable OER activities of SUNOE by preventing restack of ultrathin-nanosheets.

Conclusions

In conclusion, by governing the rates in plane and vertical to plane of SDDG through naturally consuming the precursors, the edges of nanosheets were successfully designed to overgrow. Thus a sophisticated spiral sheets structure with overgrown edges were generated, the products showed good OER performances. It's always important to carefully design the microstructure to achieve certain target, the growth mechanism here may extend to synthesize other materials. Folded single layer graphene show special band gap[40], thus we can foresee this kind of structures in graphene or TMDs may adopt new band gaps and new properties. The basic rule of nanocrystal formation is still infancy, different rules may lead to different morphologies or structures. Artfully use the basic rules may open new gate for material design.

Acknowledgements

This work was supported by NSFC (21431003, 91127040, 21221062), and the State Key Project of Fundamental Research for Nanoscience and Nanotechnology (2011CB932402)

Notes and references

Department of Chemistry, Tsinghua University, Beijing, 100084, China,

E-mail: wangxun@mail.tsinghua.edu.cn

Electronic Supplementary Information (ESI) available: [details of any supplementary information available should be included here]. See DOI: 10.1039/b000000x/

1. C. Tao, L. Jiao, O. V. Yazyev, Y.-C. Chen, J. Feng, X. Zhang, R. B. Capaz, J. M. Tour, A. Zettl, S. G. Louie, H. Dai and M. F. Crommie, *Nat. Phys.*, 2011, **7**, 616-620.
2. K. Nakada and M. Fujita, *Phys. Rev. B*, 1996, **54**, 17954-17961.
3. X. Wang, Y. Ouyang, L. Jiao, H. Wang, L. Xie, J. Wu, J. Guo and H. Dai, *Nat. Nano.*, 2011, **6**, 563-567.
4. G. Xu, J. Wang, B. Yan and X.-L. Qi, *Phys. Rev. B*, 2014, **90**, 100505.
5. X. Yin, Z. Ye, D. A. Chenet, Y. Ye, K. O'Brien, J. C. Hone and X. Zhang, *Science*, 2014, **344**, 488-490.
6. T. F. Jaramillo, K. P. Jørgensen, J. Bonde, J. H. Nielsen, S. Horch and I. Chorkendorff, *Science*, 2007, **317**, 100-102.
7. H. I. Karunadasa, E. Montalvo, Y. Sun, M. Majda, J. R. Long and C. J. Chang, *Science*, 2012, **335**, 698-702.
8. W. Zhu, Y. J. Zhang, H. Zhang, H. Lv, Q. Li, R. Michalsky, A. A. Peterson and S. Sun, *J. Am. Chem. Soc.*, 2014, **136**, 16132–16135.
9. L. Zhang, K. Liu, A. B. Wong, J. Kim, X. Hong, C. Liu, T. Cao, S. G. Louie, F. Wang and P. Yang, *Nano Lett.*, 2014, **14**, 6418-6423.
10. L. Chen, B. Liu, A. N. Abbas, Y. Ma, X. Fang, Y. Liu and C. Zhou, *ACS Nano*, 2014, **8**, 11543-11551.
11. C. Chen, Y. Kang, Z. Huo, Z. Zhu, W. Huang, H. L. Xin, J. D. Snyder, D. Li, J. A. Herron, M. Mavrikakis, M. Chi, K. L. More, Y. Li, N. M. Markovic, G. A. Somorjai, P. Yang and V. R. Stamenkovic, *Science*, 2014, **343**, 1339-1343.
12. Y. Wu, D. Wang, Z. Niu, P. Chen, G. Zhou and Y. Li, *Angew. Chem. Int. Ed.*, 2012, **51**, 12524-12528.
13. J. E. Macdonald, M. Bar Sadan, L. Houben, I. Popov and U. Banin, *Nat. Mater.*, 2010, **9**, 810-815.
14. P. Smereka, *Physica D*, 2000, **138**, 282-301.
15. Y.-I. Kwon, B. Dai and J. J. Derby, *Prog. Cryst. Growth Charact. Mater.*, 2007, **53**, 167-206.
16. F. Meng, M. S. A., F. Audrey and J. Song, *Acc. Chem. Res.*, 2013, **46**, 1616-1626.
17. S. A. Morin, A. Forticaux, M. J. Bierman and S. Jin, *Nano. Lett.*, 2011, **11**, 4449-4455.
18. A. Zhuang, J. J. Li, Y. C. Wang, X. Wen, Y. Lin, B. Xiang, X. Wang and J. Zeng, *Angew. Chem. Int. Ed.*, 2014, **53**, 6425-6429.
19. T. P. Schulze and R. V. Kohn, *Physica D*, 1999, **132**, 520-542.
20. B. Y. Xia, H. B. Wu, X. Wang and X. W. Lou, *Angew. Chem.*, 2013, **125**, 12563-12566.
21. B. Y. Xia, Y. Yan, X. Wang and X. W. Lou, *Mater. Horiz.*, 2014, **1**, 379-399.
22. R. Ma, Z. Liu, K. Takada, K. Fukuda, Y. Ebina, Y. Bando and T. Sasaki, *Inorg. Chem.*, 2006, **45**, 3964-3969.
23. J. R. Neilson, J. A. Kurzman, R. Seshadri and D. E. Morse, *Chem. Eur. J.*, 2010, **16**, 9998-10006.
24. R. Subbaraman, D. Tripkovic, K.-C. Chang, D. Strmcnik, A. P. Paulikas, P. Hirunsit, M. Chan, J. Greeley, V. Stamenkovic and N. M. Markovic, *Nat. Mater.*, 2012, **11**, 550-557.
25. M. Gao, W. Sheng, Z. Zhuang, Q. Fang, S. Gu, J. Jiang and Y. Yan, *J. Am. Chem. Soc.*, 2014, **136**, 7077-7084.
26. A. J. Bard, *J. Am. Chem. Soc.*, 2010, **132**, 7559-7567.
27. M. W. Louie and A. T. Bell, *J. Am. Chem. Soc.*, 2013, **135**, 12329-12337.
28. Q. Wang and D. O'Hare, *Chem. Rev.*, 2012, **112**, 4124-4155.
29. F. Song and X. Hu, *Nat. Commun.*, 2014, **5**, 4477.

30. M. J. Bierman, Y. K. Lau, A. V. Kvit, A. L. Schmitt and S. Jin, *Science*, 2008, **320**, 1060-1063.
31. A. Indra, P. W. Menezes, N. R. Sahraie, A. Bergmann, C. Das, M. Tallarida, D. Schmeißer, P. Strasser and M. Driess, *J. Am. Chem. Soc.*, 2014, **136**, 17530-17536.
32. C. C. McCrory, S. Jung, J. C. Peters and T. F. Jaramillo, *J. Am. Chem. Soc.*, 2013, **135**, 16977-16987.
33. W. Ma, R. Ma, C. Wang, J. Liang, X. Liu, K. Zhou and T. Sasaki, *ACS Nano*, 2015, **9**, 1977-1984.
34. X. Long, J. Li, S. Xiao, K. Yan, Z. Wang, H. Chen and S. Yang, *Angew. Chem. Int. Ed.*, 2014, **53**, 7584-7588.
35. C. C. L. McCrory, S. Jung, I. M. Ferrer, S. Chatman, J. C. Peters and T. F. Jaramillo, *J. Am. Chem. Soc.*, 2015.
36. F. Song and X. Hu, *J. Am. Chem. Soc.*, 2014, **136**, 16481-16484.
37. Y. Surendranath, M. W. Kanan and D. G. Nocera, *J. Am. Chem. Soc.*, 2010, **132**, 16501-16509.
38. S. Gao, Y. Sun, F. Lei, L. Liang, J. Liu, W. Bi, B. Pan and Y. Xie, *Angew. Chem. Int. Ed.*, 2014, **53**, 12789-12793.
39. N. Danilovic, R. Subbaraman, K. C. Chang, S. H. Chang, Y. Kang, J. Snyder, A. P. Paulikas, D. Strmcnik, Y. T. Kim, D. Myers, V. R. Stamenkovic and N. M. Markovic, *Angew. Chem. Int. Ed.*, 2014, **53**, 14016-14021.
40. H. Schmidt, J. C. Rode, D. Smirnov and R. J. Haug, *Nat. Commun.*, 2014, **5**, 5742.